Study on interaction aerodynamics of vehicle-bridge system under wind actions

J.D. YAU
Department of Architecture
Tamkang University
No.151, Yingzhuan Rd., Tamsui Dist., New Taipei City 25137
TAIWAN
jdyau@mail.tku.edu.tw

Shyh-Rong KUO

Department of Harbor and River Engineering,
National Taiwan Ocean University, Keelung 20224,
TAIWAN

Abstract: - In this study, a computational framework for performing vehicle-bridge interaction dynamics in cross winds was presented using iterative method. To investigate the interaction aerodynamics of a vehicle running on a bridge under cross wind actions, a 3D finite element model of a cable-stayed bridge subjected to moving vehicles is represented. Here, the cross winds including both steady and unsteady aerodynamic forces acting on the vehicle-bridge system are generated using spectral representation method and simulated (measured) aerodynamic coefficients along the bridge in the temporal and spatial domain. With the simulated wind forces, the vehicle-bridge system in cross winds can be composed into two subsystems: bridge-wind subsystem and vehicle-wind subsystem, and then an iterative schemes is employed to compute the interaction response between the two subsystems. By the present vehicle-bridge-wind coupling model, the aerodynamic response of a vehicle running on a cable-stayed bridge in cross winds will be presented in numerical examples.

Key-Words: - interaction aerodynamics; iterative method; vehicle-bridge system; wind engineering..

1 Introduction

The wind-induced collapse of long-span cable-supported bridges has attracted attention of bridge engineers to consider the influence of aerodynamic forces on stability of long span bridges in design stage, one of significant examples is the Tacoma Narrows Bridge destructed by mild winds in 1940 (Rocard 1957). Over the past five decades, many researchers and scientists have contributed their efforts to studying the aerodynamic vibration of cable-supported bridges. Davenport et al. (1962, 1982, 1990, 2002) and Scanlan et al. (1971, 1996, 1999) are the pioneers in developing fundamental theory of wind engineering and they have laid the foundation of wind-induced vibrations of engineering structures, such as long-span bridges and slender skyscrapers (King 2003; Miyata 2003). Due to the nonlinear and motion-dependent nature of wind loadings, the aerodynamic analysis of wind-induced response for cable supported bridges involves a tremendous amount of computations. Considering interaction effects of wind-vehicle-bridge system, Xu *et al*. (2003, 2004, 2006) adopted a 3D finite element model to investigate the aerodynamic response of suspension bridges and cable-stayed bridges carrying a train or road cars running over bridge deck under the action of high winds. In their study, the wind forces exerted on the suspension bridge are generated by computer simulations with measured aerodynamic coefficients and flutter derivatives. They concluded that the bridge motions induced by high winds might significantly affect the running safety of the train and the riding comfort of passengers. Cai and Chen (2004) presented a framework of dynamic analysis of coupled 3D vehicle–bridge system under strong winds to investigate the effects of driving speeds on dynamic performance of the vehicles as well as the bridge. Their results indicated that driving speeds of moving vehicles mainly affect the vehicle's vertical relative response while have insignificant effect on the rolling response of vehicles. Considering difficulties in measuring aerodynamic coefficients of moving train cars on bridge deck, Li et al. (2005) adopted the cosine rule to simulate the aerodynamic

coefficients of the moving coaches with yawing effect.

In this study, an iteration-based numerical algorithm will be presented for computing the response of the vehicle-bridge interaction (VBI) system caused by the simultaneous action of wind loads and moving vehicular loads. The wind loads acting on the bridge deck and car body are generated in the time domain by digital simulation techniques that can account for the spatial correlation of stochastic wind velocity field. The aerodynamic coefficient curves for the lift force and moment on the deck section are related to the angle of attack (Simiu and Scanlan 1996). With motion-dependent nature of aerodynamic forces, a finite element modelling of a two-span cable-stayed bridge will be employed to study the aerodynamic response of wind-vehicle-bridge interaction system. Then the vehicle-bridge equations of motion with aerodynamic terms are discretized by Newmark's β method (Newmark 1959) in the time domain and solved using incremental-iterative procedure.

2 Theoretical formulation

The interaction dynamic of moving vehicles on a bridge under wind actions, the wind loads acting on the vehicle-bridge system includes both steady and unsteady aerodynamic forces in the time domain that can takes into account the effects of moving speed and the spatial correlation of the vehicles with wind forces on the bridge. To simplify the wind-vehicle-bridge dynamic analysis, the following assumptions are considered in the modelling of the vehicle-bridge system in this study:

(1) 3D Bernoulli-Euler beam-column elements are used to model the bridge deck and tower of the cable-stayed bridge studied herein.
(2) The road vehicles running on the bridge are assumed to travel at a constant speed, and the vehicle is regarded as a rigid car body supported by spring-damper units.
(3) The interactions of the vehicle–bridge system are regarded as no separation and side slipping of the wheels of running vehicles.
(4) The vehicle accidents running on bridge deck, such as overturning and lateral sliding, would be excluded in the present investigations.

With the assumption (1) described above, the two-span cable-stayed bridge shown in Fig. 1 is simulated by finite element modeling. The three major components of the bridge modeled by finite elements are described as: (1) The bridge deck is modeled as a number of beam-column elements incorporating all the axial and inertial properties. (2) Each of the towers is modeled by a number of beam-column elements with the axial and flexibility. (3) Each stay cable is represented as a two-node bar or truss element of which the axial stiffness is related to the axial tension. The axial bar element considering the sagging effect caused by self-weight is used to represent the curved cable, for which the equivalent modulus E_{eq} is given by Ernst as

$$E_{eq} = \frac{E_s}{1 + \left[\dfrac{(w_c L_h)^2 (T_i + T_f) E_s A_c}{24 (T_i T_f)^2} \right]} \tag{1}$$

where E_s is the elastic modulus, L_h the horizontal projected length, w_c the weight per unit length, A_c the cross-sectional area, and T_i the initial cable tension resulting from the dead loads of the bridge and T_f the final cable tension caused by the real acting loads including vehicular loads and wind actions. The equation of motion of the whole bridge and vehicle under wind actions are written as

$$\begin{aligned} &[m_b]\{\ddot{u}_b\} + [c_b]\{\dot{u}_b\} + [k_b]\{u_b\} \\ &= \{p_{b,w}\} - \{f_c\} \\ &[m_c]\{\ddot{u}_c\} + [c_c]\{\dot{u}_c\} + [k_c]\{u_c\} \\ &= \{p_{c,w}\} + \{p_c\} + \{f_c\} \end{aligned} \tag{2}$$

where $[m_b]$, $[c_b]$, $[k_b]$ denote the mass, damping, and stiffness matrices, $\{u_b\}$ the displacements of the beam element, $\{p_{b,w}\}$ nodal aerodynamic forces acting on the beam element, and $\{f_c\}$ the contact forces existing between the vehicle system and the beam element. Also, $[m_c]$, $[c_c]$, $[k_c]$ denote the mass, damping, and stiffness matrices of the sprung mass, $\{u_c\}$ the vertical deflections of the wheel and sprung masses, and $\{p_{c,w}\}$ aerodynamic forces acting on the moving vehicles. Here, the aerodynamic force vectors of $\{p_{b,w}\}$ and $\{p_{c,w}\}$ will be described in detail in Section 3.

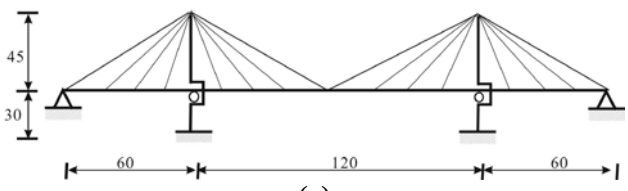

(a)

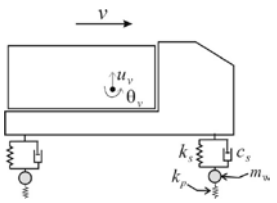

(b)

Fig. 1. VBI model of cable-stayed bridge and truck

3. Simulation of wind loads

Wind-induced vibration of moving vehicles on cable-stayed bridges are of concerns in this study. In this section, the wind loads acting on the vehicle-bridge system will be presented. The aerodynamic coefficient curves for the lift force and moment on the deck section are related to the angle of attack (Simiu and Scanlan 1996). The wind loads acting on the vehicle-bridge system are generated in the time domain by digital simulation techniques that can account for the spatial correlation of stochastic wind velocity field. Then an incremental iteration-based computational framework will be presented for dynamic analysis of the wind-vehicle-bridge system.

3.1 Wind loadings on the bridge deck

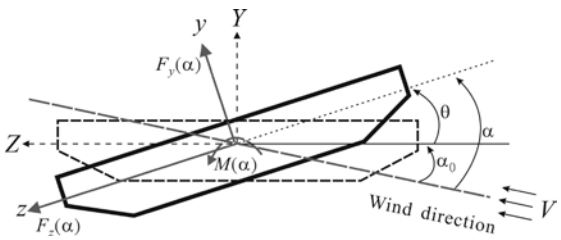

Fig. 2 Wind loads acting on the bridge deck section.

Figure 2 shows lateral wind load acting on the bridge deck with a mean velocity V and incident angle α_0. As indicated, the effective angle α of attack along the oncoming wind flow can be expressed as $\alpha(x,t)=\alpha_0+\theta(x,t)$. Since only the vertical and torsional vibrations of the beam are concerned, the lateral vibration of the beam caused by the aerodynamic drag force will be ignored. The *aerodynamic lift force* and *pitching moment* acting on the bridge deck can be expressed in terms of α as follows:

$$F_y(\alpha)=\frac{\rho V^2 B}{2}C_y(\alpha),\ F_z(\alpha)=\frac{\rho V^2 D}{2}C_z(\alpha),$$
$$M(\alpha)=\frac{\rho V^2 B^2}{2}C_M(\alpha),\qquad V=V_0+w \tag{3}$$

where V_0 = velocity of mean wind, v_w = velocity of fluctuating wind, ρ = the air density, B = bridge deck width, D = bridge deck depth, C_z = aerodynamic lift coefficient, C_y = aerodynamic lateral coefficient, and C_M = aerodynamic moment coefficient. In this study, the aerodynamic coefficients of drag (Cy), lift (Cz) and moment (C_M) of the bridge are given as: C_D = 1.18, C_L = 0.21, and C_M = 0.12 [Xu 2003], respectively.

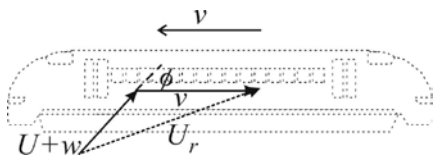

Fig. 3 Relative wind velocity and natural wind velocity to a moving vehicle

3.2 Simulation of quasi-steady aerodynamic forces on moving vehicle

Figure 3 shows the wind load model acting on a running vehicle with a mean velocity U and turbulent velocity w. The *aerodynamic forces* and *moments* acting at the mass centre of the moving vehicle are expressed as:

$$F_S=\frac{\rho A_S U_r^2}{2}C_{cS}(\varphi),M_Y=\frac{\rho A_S d_e U_r^2}{2}C_{cY}(\varphi)$$
$$F_L=\frac{\rho A_T U_r^2}{2}C_{cL}(\varphi),M_P=\frac{\rho A_T h_v U_r^2}{2}C_{cM}(\varphi) \tag{4}$$
$$U_r=\sqrt{\left[v+U\cos\phi\right]^2+\left[(U+w)\sin\phi\right]^2}$$
$$\tan\varphi=\frac{(U+w)\sin\phi}{v+U\cos\phi}$$

where ρ is the air density (= 1.2kg/m^3); A_S is the side surface area of the vehicle; A_T is the top surface area of the vehicle; d_e is the reference eccentricity of aerodynamic yawing moment about the mass centre; h_v is the reference height of vehicle's mass center; C_{cS} is aerodynamic coefficient of vehicle's side; C_{cL} is aerodynamic lift coefficient; C_{cP} is aerodynamic ralling moment coefficient; $\phi\left(=\arctan(U/v)\right)$ is yaw angle (see Fig. 3); U_r is the *relative* wind velocity around the vehicle moving at speed v; and w represent the turbulent wind speed component

will be defined in Section 3.3. The corresponding aerodynamic coefficients of side, lift, and rolling moment of a moving truck are C_{cS}=0.3, C_{cL}=0.25, and C_{cM}=0.3 [Baker 1991], respectively.

3.3 Simulation of turbulent wind velocity

To perform the interaction analysis of a maglev vehicle traveling over guideway under oncoming wind flows in the time domain, the following simplified spectral representation of turbulent wind (Xu et al. 2003) is employed to generate the time history of turbulent airflow velocity $w_j(t)$ in mean wind flow direction (lateral) at the jth point on the suspended beam as:

$$w_j(t) = \sqrt{2(\Delta\omega)}\sum_{n=1}^{j}\left[\sum_{i=1}^{N_f}\sqrt{S_w(\omega_{ni})}G_{jn}(\omega_{ni})\cos(\omega_{ni}t+\psi_{ni})\right] \quad (5)$$

where $j = 1, 2, ..., N_s$, N_f is the total number of frequency intervals represented by a sufficiently large number; N_s is the total number of points along the guideway to simulate; $S_w(\omega)$ is the spectral density of turbulence in along-wind direction (Kaimal's longitudinal wind spectrum); ψ_{ni} is a random variable uniformly distributed between 0 and 2π; $\Delta\omega = \omega_{up}/N_f$ = the frequency increment; ω_{up} is the upper cut-off frequency with the condition that the value of $S_w(\omega)$ is less than a pre-set small number ε when $\omega > \omega_{up}$; and the related wind spectrums used in Eq. (5) are given by

Horizontal wind spectrum

$$S_H(\omega) = \frac{200\times\bar{U}^2}{\left[1+50\frac{\omega}{2\pi}\left(\frac{z}{V_0}\right)\right]^{5/3}}\left(\frac{z}{V_0}\right) \quad (6a)$$

Lateral wind spectrum

$$S_L(\omega) = \frac{15\times\bar{U}^2}{\left[1+9.5\frac{\omega}{2\pi}\left(\frac{z}{V_0}\right)\right]^{5/3}}\left(\frac{z}{V_0}\right) \quad (6b)$$

Vertical wind spectrum

$$S_V(\omega) = \frac{3.36\times\bar{U}^2}{\left[1+10\frac{\omega}{2\pi}\left(\frac{z}{V_0}\right)\right]^{5/3}}\left(\frac{z}{V_0}\right) \quad (6c)$$

with the steady wind speed of $\bar{U} = \frac{KV_0}{\ln(z/z_0)}$ and

$$G_{jn}(\omega) = \begin{cases} 0 & 1 \le j < n \le N_s \\ C^{|j-n|} & n = 1, n \le j \le N_s \\ C^{|j-n|}\sqrt{1-C^2} & 2 \le n \le j \le N_s \end{cases} \quad (7)$$

with $C = \exp\left(\frac{-\lambda\omega\times\ell_{jn}}{2\pi V_0}\right)$. Here, V_0 = mean velocity of wind at height z, $\bar{U}$ stands for the shear velocity of airflow related to von Karman's constant K = 0.4 and the ground roughness z_0; λ is an exponential decay factor taken between 7 and 10; ℓ_{jn} is the distance between the simulated points j and n; and $C^{|j-n|}$ is the coherence function between points j and n (Xu et al. 2003). In this article, the following wind parameters are used: z = 30m, z_0 = 0.012 for open site, and λ = 7. Figure 4 shows the time history of fluctuating wind velocities generated by Eq. (5) in the horizontal, lift and lateral directions at x = 80m, respectively.

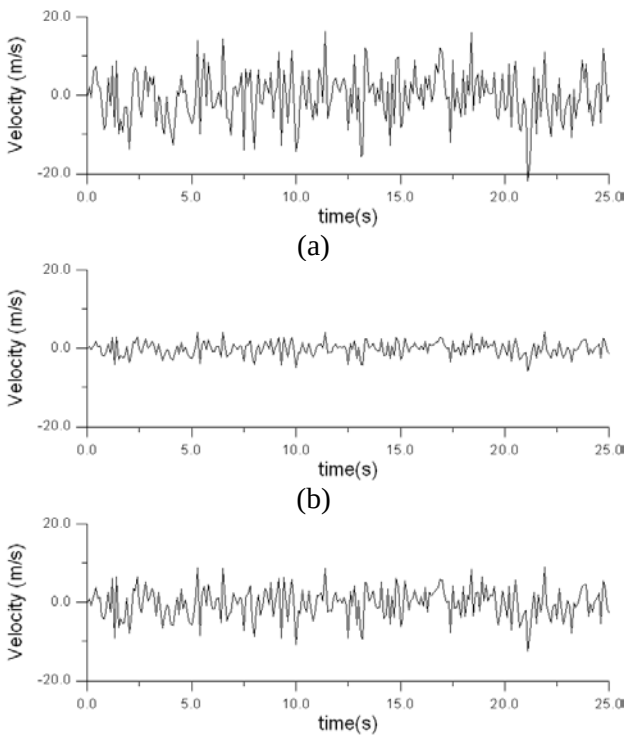

Fig. 4 Simulation of turbulent wind velocities at x = 80m. (a) Horizontal; (b) Lift; (c) Lateral.

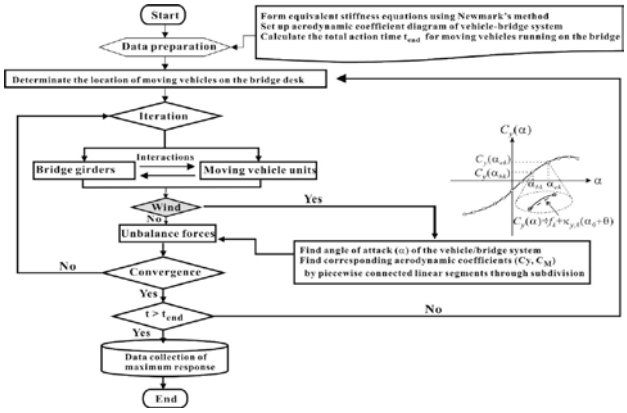

Fig. 5 Analysis procedure of nonlinear incremental-iterative method

To investigate the dynamic response of the vehicle-bridge system under wind actions, Fig. 5 shows the analysis procedure of the wind-vehicle-bridge system based on incremental-iterative approaches. Here, the nonlinear aerodynamic curves are simulated by a sequence of piecewise connected linear segments for time history response analysis of the VBI system under the action of wind loads.

4 Numerical Illustrations

As shown in Fig. 1, the bridge deck is supported by a roller at the connection with the pylon. The pylon is made of concrete with elastic modulus E_c = 35GPa and density ρ_c = 2.4t/m^3, and the steel bridge deck and stay cable with E_s = 210GPa and ρ_s = 7.8t/m^3. Rayleigh damping is assumed for the bridge with a damping ratio of 2.5%. For the sectional properties of the cable-stayed bridge, the following data are adopted in analysis: (1) cross-sectional area of the bridge deck A_b = 1.8m^2, (2) cross-sectional area of the pylon A_p = 42m^2, (3) cross-sectional area of cables A_c = 0.008 m^2, (4) moment of inertia of the bridge deck I_{bY} = 3.0m^4, I_{bZ} = 12m^4, J = 10m^4, and (5) moment of inertia of the pylon I_p = 36.28 m^4.

Considering a raw of identical moving road cars with axle-interval of 6m moving on the bridge, according to empirical formula by the Ministry of Transportation in Taiwan, the safety interval between two moving cars at the same lane of highway is estimated as v - 20 (m), in which the moving speed v is represented by km/h. The following data are used: (1) mass of the road car M_v = 5t, (2) pitching moment of inertia = 15m^4, (3) suspension unit: k_s = 480kN/m, c_s = 8.5 kN-s/m. The angle of attack ϕ = 36° of wind flow on the running cars, and α_0 = 18° on the bridge deck. By eigenvalue analysis, the vertical, lateral, and torsional frequencies of vibration solved for the bridge are: (1) 1.96Hz for vertical frequency, (2) 4.93Hz for lateral frequency, and (3) 15.7Hz for torsional frequency, respectively.

In the following numerical illustrations, two types of traffic flows are considered. The first one is the vehicles running on the bridge at one lane with one directional way, and the other one is the vehicles traveling on the bridge with two directional ways at different lanes. Moreover, two moving speeds, i.e., 15m/s (=54km/h) and 25m/s (= 90km), are considered for the running vehicles, respectively.

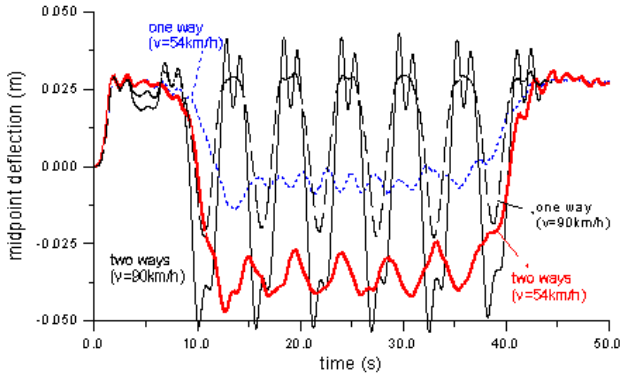

Fig. 6 Time history response of vertical midpoint deflection of the bridge

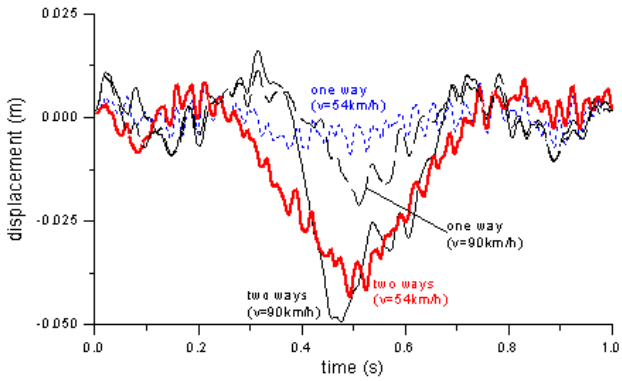

Fig. 7 Time history response of vertical displacement of road cars

Figures 6 shows the time-history midpoint displacement response of the bridge. As indicated, the higher speeds of the sequential vehicles moving with two directional traffic flows may result in larger bridge response. On the other hand, Fig. 7 draws the time-history displacement response of the specific vehicle during the period when the road car is traveling on the bridge. As the road car moves on the bridge with lower speeds, it may spend more time passing through the long-span bridge. Thus it experiences more small fluctuating excitations (see

ISBN: 978-1-61804-268-2

Fig. 6) transferring from the vibrating bridge deck induced by wind actions. But for the case of the serial vehicles moving at higher speeds, the dynamic response of the running vehicles becomes rather significant due to the significant oscillations of bridge vibration shown in Fig. 6.

6 Concluding remarks

In this study, a computational framework based on FE modelling for wind-vehicle–bridge system was established and solved using an incremental-iterative approach. The numerical studies demonstrated that the effect of two directional vehicles running on the bridge deck at different lanes is crucial to the VBI system under wind actions. With the present computational framework of wind-vehicle-bridge system, further investigation of vehicles running on bridges, such as overturning and lateral sliding, can be studied.

Acknowledgement

This research was partially supported by the Ministry of Science and Technology in Taiwan through the Taiwan-Czech joint project with the Grants: 102-2923-E-032-002-MY3.

References:

[1] Baker C.J. (1991). Ground vehicles in high cross winds. Part II: unsteady aerodynamic forces. J Fluids Struct (5), 91–111.

[2] Bryja, D., Sniady, P. (1998), Stochastic nonlinear vibrations of highway suspension bridge under inertial sprung load. J. Sound and Vibr. 216(3), 507-519.

[3] Cai, C.S., Chen, S.R. (2004). Framework of vehicle–bridge–wind dynamic analysis, J. Wind Eng. and Ind. Aerodyn. 92, 579-607.

[4] Cheng, J., Jiang, J.J., Xiao, R.C., Xiang, H.F. (2003), Series method for analyzing 3D nonlinear torsional divergence of suspension bridges, Computers and Structures 81, 299–308.

[5] Davenport, A.G. (1962), Buffeting of a suspension bridge by storm winds. ASCE J. Struct. Div. 88, 233-264.

[6] Davenport, A.G., King, J.P.C. (1982), The incorporation of dynamic wind loads into the design specifications of long span bridges. Proc. of the ASCE Fall Convention & Structures Congress, New Orleans, LA.

[7] Davenport, A.G., King, J.P.C. (1990), The influence of topography on the dynamic wind loading of long span bridges. J. Wind Eng. and Ind. Aerodyn. 36, 1373-1382.

[8] Davenport, A.G. (2002), Past, present and future of wind engineering. J. Wind Eng. and Ind. Aerodyn. 90, 1371-1380.

[9] Ernst, J.H. (1965), Der E-modul von seilen unter Berucksichtigung des durchhanges, Bauingenieur 40 (2) 52–55.

[10] Hayashikawa, T. (1997), Torsional vibration analysis of suspension bridges with gravitional stiffness. J. Sound and Vibr. 204(1), 117-129.

[11] King, J.P.C. (2003), The foundation and the future of wind engineering of long span bridges-the contributions of Alan Davenport. J. Wind Eng. and Ind. Aerodyn. 91, 1529-1546.

[12] Kuo, W.W. , Xu, Y.L. (2006), Safety analysis of moving road vehicles on a long bridge under crosswind. ASCE J. Eng. Mech. 132(4), 438-446.

[13] Li, Y.,Qiang, S.Q., Liao, H., Xu, Y.L. (2005) Dynamics of wind–rail vehicle–bridge systems, J. Wind Eng. and Ind. Aerodyn. 93, 483-507.

[14] Miyata, T. (2003), History view of long-span bridge aerodynamics. J. Wind Eng. and Ind. Aerodyn. 91, 1393-1410.

[15] Newmark, N.M. (1959), A method of computation for structural dynamics. ASCE J. Eng. Mech. Div. 85(1), 67–94.

[16] Rocard, Y.,(1957), Dynamic Instability, Frederick Ungar Publishing Company, New York.

[17] Scanlan, R.H., Tomko, J.J. (1971), Airfoil and bridge deck flutter derivatives. ASCE J. Eng. Mech. Div. 97, 1717-1737.

[18] Simiu, E., Scanlan, R.H. (1996), Wind Effects on Structures-Fundamentals and Applications to Design, 3rd Ed., John Wiely & Sons, Inc., New York.

[19] Scanlan, R.H. (1996), Aerodynamics of cable-supported bridges. J. Construct. Steel Res., 39(1), 51-68.

[20] Scanlan, R.H., Jones, N.P. (1999), A form of aerodynamics admittance for use in bridge aeroelastic analysis. J. Fluids and Struct. 13, 1017-1027

[21] Xu, Y.L., Xia, H., Yan, Q.S. (2003), Dynamic response of long suspension bridge to high wind and running train. ASCE J. Bridge Eng. 8, 46-55.

[22] Xu, Y.L., Zhang, N., Xia, H.(2004)Vibration of coupled train and cable-stayed bridge systems in cross winds, Eng. Struct. 26, 1389–1406.